

Noise-Directed Adaptive Remapping for Integer Optimization: from qubits to (encoded) qudits

Stuart Hadfield
USRA RIACS

NASA Quantum AI Laboratory
Moffett Field CA, USA
shadfield@usra.edu

Filip B. Maciejewski
USRA RIACS

Moffett Field CA, USA
fmaciejewski@usra.edu

Davide Venturelli
USRA RIACS

NASA Quantum AI Laboratory
Moffett Field CA, USA
dventurelli@usra.edu

Abstract—We extend Noise-Directed Adaptive Remapping (NDAR), a recently proposed heuristic meta-algorithm that leverages device noise as a computational resource, to optimization problems over discrete (integer) domains. While originally introduced for unconstrained binary optimization, the proposed generalization introduces additional gauge degrees of freedom at the logical level, such that the gauge transformation applied at each iteration is no longer unique, allowing tailoring to particular encodings or quantum hardware. We identify encoding-dependent requirements for NDAR beyond binary domains: feasibility of the noise attractor, existence of compatible gauge transformations that preserve an efficiently implementable circuit family, and a systematic way to select the transform to apply at each step. We analyze these criteria for qudit-native and for binary, one-hot, and domain-wall qubit encodings, using the Max- k -colorable subgraph problem as a running example. We demonstrate that these encodings can exhibit distinct advantages and tradeoffs when integrated within the NDAR framework, particularly in how noise-induced dynamics interact with the solution landscape and choice of encoding. Our results indicate that NDAR-guided noise considerations provide a new criterion for comparing device-level encoding choices for quantum optimization. Finally, we outline directions toward experimental realization in superconducting qudit devices and further algorithmic improvements.

Index Terms—Quantum computing, Optimization, Near-term quantum algorithms, Qudits, Superconducting cavities

I. INTRODUCTION

Noise-Directed Adaptive Remapping (NDAR) is a meta-algorithm recently proposed in [1] and demonstrated to dramatically improve the performance of quantum optimization algorithms deployed on real-world quantum hardware. The theory was developed for unconstrained binary optimization problems and quantum ansätze related to the Quantum Approximate Optimization Algorithm (QAOA) [2], [3], and a convincing experimental demonstration performed on a Rigetti Computing quantum processing unit (QPU) showing significant improvement with NDAR over use of the quantum ansatz alone [1, Fig. 2]. Given the many constraints and limitations of near-term quantum hardware [4] and algorithms [5], NDAR proposed a radically new approach to dealing with certain types of hardware noise: rather than attempting to error

correct or mitigate its effects, NDAR seeks to *exploit* noise as a potential resource leading to improved algorithm performance.

The main idea of NDAR is the following. Certain common types or components of noise cause the quantum computer to behave in a predictable way – the noise dynamics tries to steer whatever quantum computing output towards some preferred “attractor” state. For example, in systems or models where noise favors states of lower Hamming weight (excitation numbers), such as due to amplitude damping or dissipative effects, the attractor corresponds to the all zeros state. NDAR utilizes knowledge of the attractor state in combination with data drawn from noisy quantum measurements to implement mathematical operations (“gauge transforms”) that dynamically adjust how the problem is logically mapped to the quantum device. It further exploits the important observation that many quantum optimization algorithms require repeated preparation and measurement, which yields a large pool of candidate solutions that can be leveraged. Specifically, at each iteration NDAR transforms the cost Hamiltonian so as to align the noise attractor with the best candidate solution found.

Building on the results of [1], we explore how NDAR may be extended to applications beyond unconstrained binary optimization, and to more general quantum devices, including those based on d -level quantum systems (qudits). Indeed, a number of emerging quantum technologies are striving beyond considering strictly two-level quantum systems, utilizing multiple quantum levels within each quantum subsystem, i.e., *qudit*-based quantum processors [6]–[16]. Here we focus on problems over discrete domains such as \mathbb{Z}_d^n , which can be mapped directly to such systems or to qubits via different encodings, including both binary and unary variants [3], [17]. To this end we generalize NDAR beyond prior work to explicitly handle certain classes of *hard constraints* which may be given as problem input, or can arise directly from the choice of encoding. For the prototypical integer domain problems we consider, we show that qudit implementations of NDAR present several advantages

Encoding	Qudit	Binary / Gray	One-Hot	01-Hot	Domain-Wall
Qudits/Qubits per variable	1	$\lceil \log_2 d \rceil$	d	$d - 1$	$d - 1$
Probability q of valid string	$q = 1$	$q = 1$ ($d = 2^\ell$)	$q \leq 1$	$q \leq 1$	$q \leq 1$
Additional hard constraints?	No	No ($d = 2^\ell$)	Yes	Yes	Yes
$ 00 \dots 0\rangle$ attractor feasible?	Yes	Yes	No	Yes	Yes
Cost Hamiltonian / Phase Op.	2-local	$2 \lceil \log_2 d \rceil$ -local	2-local	$2(d - 1)$ -local	2-local
Mixing Operator	1-local	1-local ($d = 2^\ell$)	2-local	$(d - 1)$ -local	2-local

TABLE I: Comparison of d -level encodings on qudits and qubits for problems over \mathbb{Z}_d^n such as Max- d -colorable subgraph. Native qudit encodings exhibit "best-of-category" combination of advantageous properties over qubit ones.

over comparable qubit-based encodings; some of the key differences are summarized in Table I, with details given in Sec. III and IV. We leverage our results to give an outlook for experimental realizations in the near-term and beyond in Sec. V.

II. PRELIMINARIES

We first overview some key technical components regarding quantum optimization, and extensions to qudits, and NDAR. For simplicity we present a single overarching version of NDAR in Algorithm 1 below that subsumes prior work as special cases.

A. Combinatorial Optimization

Consider optimization problems over strings $y \in \mathbb{Z}_k^n$, where we are given some cost function $c(y)$

$$c : \mathbb{Z}_k^n \rightarrow \mathbb{R} \quad (1)$$

we seek to maximize (or minimize). The case $k = 2$ corresponds to binary optimization. The case $k > 2$ captures the case of each variable drawn from one of k possible assignments (which are identified with k integers). For simplicity we assume each variable is drawn from the same domain (same k), whereas in general they may be different, and that k is finite.

Additionally we also may be given a set $\{a_j\}$ of hard constraints $a_j : \mathbb{Z}_k^n \rightarrow \mathbb{R}$ with the requirement that

$$\forall j \ a_j(y) = 0 \quad (2)$$

must be satisfied for any valid candidate solution y ; such y are called *feasible*. While for unconstrained optimization this set is initially empty, the choice of problem encoding can nevertheless introduce hard constraints; the latter is the type of problem constraints we primarily consider in this paper. Hence we will sometimes encounter *invalid* strings in the encoded domain that do not correspond to variable assignments. For example, the $00 \dots 0$ string is invalid in a one-hot encoding of an integer variable. Invalid strings can often be efficiently 'corrected' to obtain a valid string using a fixed heuristic, though often lacking closeness guarantees. For example, for one-hot encodings, a measured string of Hamming weight greater than one could flip bits to zero until valid, say randomly, or based on the structure of the problem such as which correction is most advantageous.

For quantum optimization algorithms on qubits, such as those based on QAOA and its generalizations, variable values are typically mapped to qubit basis states $|0\rangle, |1\rangle$. The cost function is then mapped [18], [19] to a diagonal cost Hamiltonian to be maximized (or minimized):

$$H = h_0 I + \sum_i h_i Z_i + \sum_{i < j} h_{ij} Z_i Z_j + \dots \quad (3)$$

where Z_i is Pauli Z operator acting on qubit i , h_i is a local field magnitude, and $h_{ij} \in \mathbb{R}$ is interaction strength between qubits i, j . When hard constraints are present, each a_j (or a_j^2) of (2) can be similarly mapped to diagonal Hamiltonians A_j that together act to penalize infeasible or invalid states.

We give a qudit generalization of (3) in Sec. II-C.

1) *Bitflip transforms*: For qubits, consider the unitary bitflip (spin-reversal) operators $P_y = \bigotimes_{i=0}^{n-1} X_i^{y_i}$ that act to flip the $|0\rangle, |1\rangle$ basis states for each bit indicated by the bitstring $y \in \{0, 1\}^n$. For bitflip transforms we have the property $P_y^\dagger = P_y$, which will not hold for the more general gauge transformations we consider shortly.

Applying this change-of-basis to H is equivalent to changing the signs of the coefficients h_i and h_{ij} as $H \rightarrow H^y := P_y^\dagger H P_y$ with

$$H^y = P_y H P_y = h_0 I + \sum_i (-1)^{y_i} h_i Z_i + \sum_{i < j} (-1)^{y_i + y_j} h_{ij} Z_i Z_j + \dots, \quad (4)$$

and similarly for any higher order terms. This gauge transformation preserves cost Hamiltonian eigenvalues, with eigenvectors (candidate problem solutions) permuted under P_y . In particular, under this transformation the $|0 \dots 0\rangle$ state is mapped to $|y_0 \dots y_{n-1}\rangle$. Any constraint Hamiltonians A_j are also diagonal and transform in the same way as H .

For QAOA, both the standard initial state and mixing operator are invariant under P_y , and the phase operator changes only in sign of the coefficients that correspond to the changes to H , which will compile to the same circuit up to negation of the rotation angles of a subset of quantum gates.

B. Noise-Directed Adaptive Remapping (NDAR)

NDAR is a recently proposed meta-algorithm [1] that can significantly improve quantum optimization perfor-

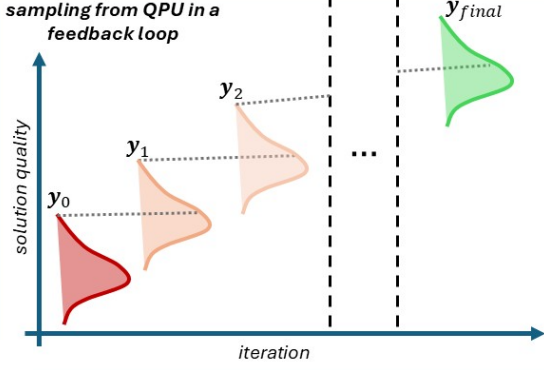


Fig. 1: Schematic illustration of NDAR: the distribution of solution costs obtained from the quantum device is iteratively improved by successive problem gauge transforms which seek to align the noise attractor with high-quality solutions; see e.g. [1, Fig. 1] for comparable results obtained from real-world quantum hardware.

mance on device implementations by exploiting rather than mitigating the effects of hardware noise. Here we recap the main ideas and requirements towards generalization. NDAR works by identifying a classical “attractor state” of the noise naturally present in the quantum processor, and then dynamically remapping how the problem is encoded on the quantum device to use the noise as an active local search heuristic. At each iteration, a gauge transform (such as the bitflip transform) is determined via data sampled from the quantum runs, adaptively selected to improve the cost value corresponding to the attractor.

Algorithm 1 NDAR for qudits or qubits (greedy remapping)

Input: $(|00\dots 0\rangle)$ is assumed feasible attractor state)

- $H_{(0)}$: cost Hamiltonian to be maximized. (Minimization case is similar).
- $\{A_i\}$: initial hard constraints that must be satisfied.
- **optimizer**: a quantum subroutine that performs a stochastic optimization of $H_{(l)}$ (gauge-transformed Hamiltonian in iteration step $l + 1$).
- gauge transformation selection rule $\mathbf{x} \rightarrow P_{\mathbf{x}}$
- M : total number of samples in each optimization step.
- **TERMINATION**: a rule specifying when to halt.

Pseudocode for iteration j :

- 1) Run **optimizer** for $H_{(j-1)}$, $\{A_i\}$. Result: M bitstrings $\{\mathbf{x}_{(j)}^i\}_{i=1}^M$.
 - 2) Discard or correct infeasible bitstrings, yielding $M' \leq M$ solutions.
 - 3) Calculate costs $\{E_{(j)}^i\} = \langle \mathbf{x}_{(j)}^i | H_{(j-1)} | \mathbf{x}_{(j)}^i \rangle_{i=1}^{M'}$.
 - 4) Select the bitstring \mathbf{x}^* such that $E_{(j)}^* = \max_i E_{(j)}^i$ (or $= \min_i E_{(j)}^i$).
if **TERMINATION**: **return** highest (lowest) energy solution found.
 - 5) Apply gauge transform $P_{\mathbf{x}^*}$ to $H_{(j-1)}$ to obtain $H_{(j)} := H_{(j-1)}^{\mathbf{x}^*} = P_{\mathbf{x}^*}^\dagger H_{(j-1)} P_{\mathbf{x}^*}$ (cf. Eq. (4)). This ensures that the transformed Hamiltonian satisfies $\langle 00\dots 0 | H_{(j)} | 00\dots 0 \rangle = E_{(j)}^*$.
 - 6) Apply $P_{\mathbf{x}^*}$ to each constraint: $A_i \leftarrow P_{\mathbf{x}^*}^\dagger A_i P_{\mathbf{x}^*}$.
 - 7) Increment j and proceed to Step 1.
-

Prior work considered NDAR for qubits in the setting of unconstrained optimization. Abstracted toward generalization, NDAR rests on four key ingredients:

- 1) **Attractor**: a noise model or device behavior with a known classical *attractor state* (e.g., $|00\dots 0\rangle$).

The attractor may follow from the noise model or be inferred empirically. For instance, any noise channel that suppresses Hamming weight makes $|00\dots 0\rangle$ the attractor, regardless of how often it is actually sampled.

- 2) **Feasibility**: the attractor must encode a *feasible solution* at every iteration.

This is automatic for unconstrained binary optimization, but is not guaranteed once hard constraints or non-trivial encodings enter the picture. Here we extend NDAR to families of constraints $\{A_i\}$ including those whose feasible sets form a transitive orbit under an efficiently constructible group action. This class includes, but is not limited to, common encodings of integer domains. For example, in one-hot encodings all feasible codewords lie in a single orbit of an easily implemented permutation. In contrast, for the Maximum Independent Set problem the feasible set is not generally a transitive orbit under simple permutations, and as a result we cannot construct a set of gauge transformations satisfying all of our criteria in a straightforward way.

- 3) **Gauge selection**: each accepted measurement outcome must *uniquely determine*, through a specified selection rule, a gauge transformation $x \mapsto P_x$ that maps the attractor to the target string.

For binary optimization, the bitflip (automorphism) group acts *simply transitively* on the set of bitstrings, so the best sampled solution unambiguously specifies the next gauge. Beyond binary, this correspondence breaks and the mapping must be specified.

To choose the target string at each iteration here we follow the *greedy choice rule* [1] of mapping to the best solution found at the current iteration.

- 4) **Practical circuit remappings**: the derived quantum circuit must transform in a way under the gauge that preserves sufficient structure of the ansatz so as to not introduce unscalable overheads in the iterative procedure. This is ultimately an operational constraint that will depend on implementation details (such as compilation efficiencies) as well as hardware specifications and noise.

Bitflip gauges leave QAOA circuits identical up signs of (single-qubit) rotations: hence the noise profile is preserved across iterations. More general transformation may introduce new terms or dramatically reshape the circuit, breaking this property.

We show the steps of the simplest version of the NDAR in Algorithm 1, presented generally to account for the extensions to qudits and encoded problems of Sec. II-C. Our Steps 2 and 6 are new, to explicitly deal with infeasible strings in cases of problems with hard constraints. Note that Algorithm 1 assumes the attractor state to be $|00\dots 0\rangle$, encoding a feasible state.

Remarks on hard constraints: Different approaches exist for extending quantum optimization algorithms to problems with hard constraints, with different tradeoffs. A common approach is to incorporate constraints directly into a modified cost Hamiltonian $H' = H + \lambda \sum_j A_j^2$ that contains sufficiently large penalty terms as controlled by the parameter λ . This approach still yields infeasible solutions with nonnegligible probability. Alternatively, one can avoid this overhead by instead incorporating constraints into the design of mixer operators and initial state such that the algorithm is restricted to the subspace of feasible states [3]. Our assumption that the attractor state is feasible, together with the property that our modified algorithm selects only gauge transforms to other feasible states, imply that our generalization of NDAR is compatible with both approaches.

C. Quantum Optimization with Qudits

Abstractly, the domain \mathbb{Z}_d^n naturally corresponds to state space of n -many d -level qudits, in the same way as for binary domains and qubits. Hence, irrespective of what lower level encodings or physical devices are utilized, one may first proceed at the level of *logical qudits*, where each \mathbb{Z}_d is mapped to the basis states $\{|0\rangle, |1\rangle, \dots, |d-1\rangle\}$. This idea was applied, for instance, in various Quantum Alternating Operator Ansatz constructions of [3]. QAOA for qudits has been further considered in [16], [20]–[24], among other works.

As with qubits, different possible quantum circuit ansatz are possible for qudit-based approaches to combinatorial optimization. Here we briefly review QAOA, consisting of three main components: an initial state, along with so-called phase and mixing operators which are applied in alternation, and then the state is measured to return a candidate problem solution. To implement QAOA at the logical qudit level we may consider, for instance, the initial state

$$\left(\frac{1}{\sqrt{d}}(|0\rangle + |1\rangle + |2\rangle + \dots + |d-1\rangle)\right)^{\otimes n} \quad (5)$$

which gives the usual equal superposition over all states; other initial states are possible [3]. The phase operator is

$$U_P = \exp(-i\theta H),$$

where H is the cost Hamiltonian satisfying $H|y\rangle = c(y)|y\rangle$. For mixing operator U_M , different choices are possible [21], in particular such that the design criteria of [3] is satisfied. In general some operator of the form

$$U_M = \bigotimes_{j=1}^n \exp(-i\beta B_j)$$

suffices where each B_j acts nontrivially on (typically) a single logical qudit. For unconstrained problems over integers, B_j can be set to be (Hermitian combinations of) left- or right-shift operators, which generalize the usual

transverse field $B_j = X$ mixer for qubits. For a d -level qudit we may generalize the qubit Pauli operators to become the shift and clock operators

$$X_d|j\rangle = |j+1 \pmod{d}\rangle, \quad Z_d|j\rangle = \omega^j|j\rangle \quad (6)$$

with $\omega_d = e^{2\pi i/d}$, which satisfy the Weyl commutation relation $ZX = \omega XZ$; when d is clear from context we omit their subscripts. An important difference is that these operators are no longer Hermitian for $d > 2$. Nevertheless a mixer can be constructed using $B_j = (X + X^\dagger)/2$ for each qudit [3], [21]. We emphasize that the mixer U_M may be specified and transformed at the logical level, and then mapped to appropriate gates implementing it once a hardware encoding is specified.

III. NDAR FOR QUDITS

Here we present our extension of NDAR to qudit-based quantum hardware, previously briefly teased in [16]. In what follows we significantly expand upon the prior work. We first motivate our construction by discussing how amplitude damping noise generalizes to qudit systems. For sufficiently low temperature the attractor state again approaches $|00\dots 0\rangle\langle 00\dots 0|$, while more generally it is a mixed thermal state dominated by low excitation number components.

A. Generalized amplitude damping channels

Consider for the moment a single system qudit Hamiltonian of the form $\tilde{H} = \sum_{j=0}^{d-1} E_j|j\rangle\langle j|$, with $0 = E_0 < E_1 < \dots < E_{d-1}$; i.e., the spectrum of \tilde{H} defines the computational basis and is nondegenerate. For qubits ($d = 2$), amplitude damping models energy relaxation $|1\rangle \rightarrow |0\rangle$ with some probability p (e.g., spontaneous emission), which at zero temperature is described by the Kraus operators

$$K_0 = |0\rangle\langle 0| + \sqrt{1-p}|1\rangle\langle 1|, \quad K_1 = \sqrt{p}|0\rangle\langle 1|. \quad (7)$$

For qudits, different generalizations are possible; for example, damping channels may allow limited or arbitrary downward jumps in energy. Generally amplitude damping means population flows downward in energy $|d-1\rangle \rightarrow |d-2\rangle \rightarrow \dots \rightarrow |1\rangle \rightarrow |0\rangle$. This type of channel is important for modeling various types of systems including for example leakage and relaxation in transmons, and loss in truncated bosonic channels. Generally, amplitude damping can result from coupling to a bath with modes that can absorb the qudit's transition energy (electromagnetic modes, phonons, other two-level defects, etc.), turning excited-state energy into environmental excitations. This includes spontaneous emission into electromagnetic modes or phonons, dielectric loss from a bath of two-level systems, and thermal excitations, among other physical mechanisms.

a) *Zero-temperature amplitude damping*: At zero temperature, the bath is its ground state (cannot provide energy), hence only downward jumps are allowed. Consider a single oscillator-like qudit and let $\eta = \exp(-\kappa t)$ denote the transmissivity over the channel time t , so that $\gamma = 1 - \eta$ is the probability that each individual excitation is lost (such as by single boson emission in harmonic oscillators). Then the number of lost excitations is binomially distributed, with the probability of the transition $|j\rangle \rightarrow |j-i\rangle$ given by $\binom{j}{i}(1-\gamma)^{j-i}\gamma^i$, and so one defines the amplitude damping channel [25]–[27] by the Kraus operators

$$K_i = \sum_{j=i}^{d-1} \sqrt{\binom{j}{i}(1-\gamma)^{j-i}\gamma^i} |j-i\rangle\langle j|, \quad (8)$$

for $i = 0, 1, \dots, d-1$, derived as a truncated bosonic pure-loss channel. In the short-time limit we have $\gamma \simeq \kappa t$ and the dominant transition from each basis state is $|j\rangle \rightarrow |j-1\rangle$ with probability $j\kappa t + O(t^2)$, corresponding to adjacent transition rate $\Gamma_j^- = j\kappa$. Generally this model allows all downward transitions, is non-unital, and has density matrix fixed point $|0\rangle\langle 0|$. For n qudits each under the action of this channel, the fixed point is then $|00\dots 0\rangle\langle 00\dots 0|$ in the sense that $\Lambda^\ell(\rho) \rightarrow |00\dots 0\rangle\langle 00\dots 0|$ up to phase as $\ell \rightarrow \infty$, for $\Lambda(\rho) := \sum_{i=0}^{d-1} K_i \rho K_i^\dagger$. Hence for qudits under the amplitude damping noise of Eq. 8 we expect the output distribution to be skewed toward states of low excitation number, analogous to the skew towards states of low Hamming weight observed and exploited for qubits in [1].

b) *Finite-temperature generalizations*: At finite temperature both absorption and emission are allowed, subject to detailed-balance conditions. This models a coupling to a thermal bath.

From the continuous-time perspective, defining jump operators $L_j^- = |j-1\rangle\langle j|$ and $L_j^+ = |j\rangle\langle j-1|$ the Lindbladian becomes

$$\mathcal{L}(\rho) = \sum_{j=1}^{d-1} [\Gamma_j^- \mathcal{D}[L_j^-](\rho) + \Gamma_j^+ \mathcal{D}[L_j^+](\rho)], \quad (9)$$

where $\mathcal{D}[L](\rho) = L\rho L^\dagger - \frac{1}{2}\{L^\dagger L, \rho\}$. Assuming thermal equilibrium at inverse temperature β , from detailed balance the rates satisfy $\Gamma_j^+/\Gamma_j^- = e^{-\beta(E_j - E_{j-1})}$ such that the unique fixed point is the Gibbs state

$$\frac{e^{-\beta \tilde{H}}}{\text{Tr}(e^{-\beta \tilde{H}})} = \frac{1}{Z} \left(|0\rangle\langle 0| + e^{-\beta E_1} |1\rangle\langle 1| + e^{-\beta E_2} |2\rangle\langle 2| + \dots \right).$$

Hence, while the fixed point for each qudit is no longer $|0\rangle\langle 0|$, higher energy level components are exponentially suppressed with inverse temperature and energy.

As a discrete channel over a time step t the CPTP map is $\Lambda_t = e^{t\mathcal{L}}$. Hence for small t , the Kraus operators are now approximately

$$K_0 \approx I - \frac{t}{2} \sum_{j=0}^{d-1} (\Gamma_j^- + \Gamma_{j+1}^+) |j\rangle\langle j|,$$

$$K_j^- \approx \sqrt{\Gamma_j^- t} |j-1\rangle\langle j|, \quad K_j^+ \approx \sqrt{\Gamma_j^+ t} |j\rangle\langle j-1|,$$

which generalizes the zero temperature case above in the short-time limit. (Here we take $\Gamma_0^- = \Gamma_d^+ = 0$, whereas more general device channels may also include leakage to non-computational states [15], [28], [29].) Hence, for n qudits under finite temperature amplitude damping noise we again expect the output distribution to be skewed toward low excitation states, and so in principle exploitable by NDAR.

More generally still, one may consider distinct rates for each allowed transition between two states $|i\rangle$ and $|j\rangle$, such as for anharmonic spontaneous emission/absorption transitions in atomic systems [26]. In the short time (i.e., small Γ_j^\pm) limit single transitions between adjacent states in the ladder again dominate. In either setting the low-temperature bias toward low-energy labels remains.

B. NDAR for logical qudits

Suppose a problem on \mathbb{Z}_d^n is mapped directly to n d -level qudits (we sometimes call \mathbb{Z}_d values *colors*). We revisit the four ingredients of Sec. II-B in this setting:

- 1) **Attractor**: the qudit state $|00\dots 0\rangle$ remains the natural attractor, analogous to the qubit case. This is motivated by the generalized amplitude damping channels of Sec. III-A, which act to suppress excitation number on each qudit. Other attractors can be accommodated with minimal changes.
- 2) **Feasibility**: the attractor encodes a feasible state for unconstrained problems, as in the qubit case.
- 3) **Gauge selection**: the qubit one-to-one correspondence breaks, leaving an *exponentially large family* of gauges compatible with each sampled string.

For $d > 2$, per-qudit relabelings of the d logical levels yield $(d!)^n \gg d^n \gg 2^n$ gauge transformations. Even after fixing which level each qudit sends $|0\rangle$ to, the remaining $d-1$ levels can be permuted freely, leaving $((d-1)!)^n$ compatible gauges per sampled string instead of a unique gauge as for qubits.

Given a target string $y \in \mathbb{Z}_d^n$ we consider general gauge transformations

$$H^y := P_y^\dagger H P_y \quad (10)$$

where P_y acts to map the attractor state to y , defined here with the convention $P_y|0\rangle = |y\rangle$ such that $\langle 0\dots 0|H^y|0\dots 0\rangle = \langle y|H|y\rangle$. We require that each y determines P_y efficiently and uniquely.

- 4) **Practical circuit remappings**: the surplus gauge freedom becomes a design lever toward hardware-friendly circuits:

From the $((d-1)!)^n$ compatible gauge transforms one can *choose* $\{P_{\mathbf{y}}\}$ to be the cheapest or most convenient set to implement for the available hardware and ansatz (e.g., transpositions swapping two levels, versus cyclic shifts X_d^r of all d levels, for each qudit). The goal is to use this freedom to select gauge transforms that preserve as much circuit structure as possible, e.g. by restricting to hardware-friendly subgroups (such as cyclic shifts).

Item 3 shows that qudits come with significantly more gauge freedom than qubits, which we argue is advantageous. In particular, this allows *different sets of allowed gauge transformations to be tailored to different qudit encodings*. For example, for a single qudit, the previous and desired labels may be swapped, which doesn't affect the labels of any other levels, or a shift operator X^r can be applied for r the difference between the two values, which shifts the label of every qudit level. For hardware qudits, one can consider gauge transformations most compatible with the quantum ansatz employed as well as lower-level quantum gates. This freedom is especially important for the case of qudits encoded in qubits, where we show different encodings naturally lead to different choice gauge transformations, distinct from each other as well as from the pure qudit encoding.

Remark 1. *The set of gauge transforms often forms a subgroup of the permutation group $(S_d)^n$ on encoded basis states, though not always. For qudit shift gauges of Eq. (14) this subgroup is \mathbb{Z}_d^n (acting transitively on \mathbb{Z}_d^n by translations). More general gauge transformation rules may select different representatives from the compatible elements of $(S_d)^n$ for each target string \mathbf{y} .*

C. Example: Graph k -coloring problems

Here we consider graph coloring as a prototypical example of a problem over integers that captures the basic essence of scheduling, planning, and asset allocation problems. Deciding whether a given graph is properly k -colorable for $k \geq 3$ is a well-known NP-complete decision problem, and a variety of distinct optimization variants of this problem exist; see e.g. [3], [30].

Given an n -node graph $G = (V, E)$ and k colors $1, \dots, k$ (sometimes labeled $0, \dots, k-1$), find an assignment of colors to each node such that a particular cost function is optimized or satisfied, along with possible hard constraints that must be satisfied. Different problem variants exist related to both proper and improper colorings. A coloring is proper if no edge in the graph connects vertices of the same color, else improper. Here we use coloring to denote any possible color assignment.

Max- k -colorable subgraph problem [3], [20]: given fixed $k \geq 2$, maximize the objective function

$$c(x) = \# \text{ edges connecting differently colored vertices}$$

for all possible assignments $x \in \{1, 2, \dots, k\}^n$ of k colors to n vertices. This problem naturally generalizes

Maximum Cut which is a commonly considered application problem for quantum algorithms, and is reproduced for the case $k = 2$. Applications related to scheduling problems include variants where each node may have its own set of allowed colors, and the goal remains to minimize conflicts. Here for simplicity we consider the version as described.

Qudit encoding: Suppose we have available a quantum computer with n many (logical) k -level qudits (i.e., $d = k$). First rewrite the cost function as

$$c(x) = \sum_{(uv) \in E} \text{NEQ}(\text{col}_u(x), \text{col}_v(x)).$$

Here $\text{col}_u(x)$ denotes the function that returns the color assigned to a vertex u by a string $x \in \mathbb{Z}_k^n$, and EQ, NEQ denote the Equal and Not Equal functions, respectively. We identify these strings with basis states i.e. $|red\rangle, |green\rangle, |blue\rangle, \dots, |violet\rangle$, which we conveniently identify with integers and the qudit states

$$|0\rangle, |1\rangle, |2\rangle, \dots, |d-1\rangle, \quad (11)$$

In this representation the cost Hamiltonian becomes

$$H = |E|I - \sum_{(uv) \in E} (|00\rangle\langle 00| + |11\rangle\langle 11| + |22\rangle\langle 22| + \dots + |(d-1)(d-1)\rangle\langle (d-1)(d-1)|)$$

Here we represent the cost Hamiltonian using projector primitives [21] $\Pi_{u,v} := \sum_{j=0}^{d-1} |j\rangle\langle j|_u \otimes |j\rangle\langle j|_v = \sum_{j=0}^{d-1} |jj\rangle_{uv} \langle jj|_{uv}$. For qudits, a variety of operator bases to represent such operators and ultimately quantum gates are possible [6], [21].

Qudit-based ansatz: Given H , we can construct an ansatz such as QAOA (Sec. II-C), which may be compiled to logical or low-level qudit gates in different ways.

a) Compilation via generalized Pauli operators:

Recall Eq. (6) above. On \mathbb{Z}_d we have the identity $\delta_{x_u, x_v} = \frac{1}{d} \sum_{m=0}^{d-1} \omega^{m(x_u - x_v)}$, and so observing $Z_u^m Z_v^{-m} |j_u, j_v\rangle = \omega^{m(j_u - j_v)} |j_u, j_v\rangle$ we have $\sum_{j=0}^{d-1} |jj\rangle \langle jj|_{uv} = \frac{1}{d} \sum_{m=0}^{d-1} Z_u^m Z_v^{-m}$. Hence the cost Hamiltonian becomes

$$H = (1 - \frac{1}{d})|E|I - \frac{1}{d} \sum_{(u,v) \in E} \sum_{m=1}^{d-1} Z_u^m Z_v^{-m}, \quad (12)$$

where a Hermitian decomposition is obtained observing all terms occur in conjugate pairs $Z_u^m Z_v^{-m} + Z_u^{-m} Z_v^m$, and so the phase separator $e^{-i\gamma H}$ decomposes into commuting edge phases implementable with two-qudit controlled-phase gates.

For the mixer, the transverse field Hamiltonian generalizes to a Hermitian combination of shift operators

$$B = \sum_{v \in V} (X_v + X_v^\dagger) \quad (13)$$

of Eq. (6). As $[X, X^\dagger] = 0$, the mixer $e^{-i\beta B}$ can be implemented exactly as the product of partial mixing

terms $e^{-i\beta(X+X^\dagger)}$. The partial mixers are generally not Clifford operations, except at special angles or for special d . Nevertheless they can be easily compiled from the Fourier transform identity $FXF^\dagger = Z$ which implies $X + X^\dagger$ is diagonalized by F^\dagger . In particular, if one can implement a diagonal unitary in the Z basis then a partial mixing term can be implemented by conjugation as

$$e^{-i\beta(X+X^\dagger)} = F^\dagger \left(e^{-i\beta(Z+Z^\dagger)} \right) F.$$

b) Compilation to SUM and controlled-phase:

Consider the two-qudit controlled-phase gate which acts as $CP|a, b\rangle = \omega^{ab}|a, b\rangle$. This is a Clifford gate for prime d , and is related to the qudit SUM gate, $SUM|a, b\rangle = |a, b+a\rangle$, by conjugation with F on one qudit, $CP = (I \otimes F)SUM(I \otimes F^\dagger)$. Using these primitives and single-qudit gates [31]–[34] one can implement $e^{-i\theta(Z_u^m Z_v^{-m} + Z_u^{-m} Z_v^m)}$ with standard phase kickback: compute the modular difference into an ancilla register using SUM and inverse-SUM, apply a single-qudit diagonal phase gate on that register, and uncompute.

c) Compilation to hardware: Different low-level gate sets and primitives exist to compile the above logical operators to. SNAP and Displacement gates [35], [36] are universal for single qudit operations, and can implement multiqubit operations once augmented with entangling gates [37]–[39]. Other options include echoed conditional displacement gates [40]–[42] which use an ancilla qubit dispersively coupled to an oscillator or cavity, as well as optimized direct control-level pulses [22], [43]. We provide some further discussion in Sec. V.

Gauge transform fixing: Starting at the logical qudit level we propose the choice of gauge transformation

$$V(r) = X^{r_1} X^{r_2} \dots X^{r_n} \quad (14)$$

where $X := X_d$ is the left-shift operator and $r_u = col_u(x^*) - col_u(0)$ is defined for each qudit (integer variable) as the difference between the integer label of the best solution found at the current step and that encoded by 0. Under this choice the cost Hamiltonian (12) transforms as under $V = V(r)$ as

$$V^\dagger H V = (1 - \frac{1}{d})|E|I - \frac{1}{d} \sum_{(uv) \in E} \sum_{m=1}^{d-1} \omega^{m(r_u - r_v)} Z_u^m Z_v^{-m}.$$

Hence we see that here each Pauli term in H may be phase shifted by a d th root of unity, generalizing the sign flip case for qubits. (Similar formulas apply for higher order Pauli Z_d terms.) This choice is natural for many qudit gate sets. As we will see below, different sets of gauge transformations will be convenient when the same problem is mapped to qubits.

IV. NDAR FOR ENCODED VARIABLES

Here extend NDAR-QAOA to integer domains encoded with qubits, and consider tradeoffs in terms of suitability for NDAR and as compared to the qudit case presented

above. To illuminate these results we continue with the Max- k -colorable subgraph problem as our running example. See e.g. [3], [17] for discussion of encodings and tradeoffs. Here we focus on the main differences from the results given in Sec. III.

A. Binary qubit encoding

In binary encoding we use $\ell = \lceil \log_2(k) \rceil$ qubits per vertex to encode each color. Here we identify the logical basis states of Eq. (11) with the basis states of qubit pairs

$$|0\dots 00\rangle, |0\dots 01\rangle, |0\dots 10\rangle, \dots, |1\dots 11\rangle \quad (15)$$

with $\mathcal{E}(j) = |j\rangle_2 = |j_{\ell-1} \dots j_1 j_0\rangle$, $\sum_{i=0}^{\ell-1} j_i 2^i$. Here we assume k is a power of 2, which results in all states being valid, and in particular the usual transverse-field mixer

$$U_M = \prod_{v=1}^n \prod_{j=0}^{\ell-1} \exp(-i\beta X_{v_j}) \quad (16)$$

is appropriate, and can be implemented with ℓn single qubit (X -rotation) gates. (If $k \neq 2^\ell$, one could assign multiple strings per color, resulting in more complicated cost and mixing operators, or apply other strategies with different tradeoffs.)

For initial state, $|\psi_0\rangle = |+\rangle^{\otimes \ell n}$ encodes the equal superposition over all possible coloring assignments and is trivially prepared. The cost Hamiltonian becomes

$$H = |E| - \sum_{(uv) \in E} \sum_{j=0}^{k-1} |\mathcal{E}(j)\mathcal{E}(j)\rangle \langle \mathcal{E}(j)\mathcal{E}(j)| \quad (17)$$

which can be uniquely mapped to Pauli Z qubit operators [19]. For example, for $k = 4$ this becomes $\sum_{(uv) \in E} (\frac{3}{4}I - \frac{1}{4}Z_{u_0}Z_{v_0} - \frac{1}{4}Z_{u_1}Z_{v_1} - \frac{1}{4}Z_{u_0}Z_{v_0}Z_{u_1}Z_{v_1})$. For $k = 2^\ell$ this generalizes to k terms per edge and H becomes 2ℓ -local (i.e., its terms act on up to 2ℓ qubits).

For the phase operator $U_P = \exp(-i\gamma H)$, dropping the constant term and utilizing commutativity gives a product of k multiqubit Pauli rotations. In the standard decomposition of [44] this requires at most $|E|(k-1)$ single qubit rotations and $O(|E|\ell k)$ CNOT gates; other gate sets and optimizations are possible. Hence we see the resource requirements for QAOA for k -coloring in binary encoding are modest; in particular for $k = 4$ they are roughly double that of QAOA for MaxCut.

NDAR for binary encodings: Suppose we have used QAOA or some other suitable algorithm for obtaining a set of solution samples, and assume that the system noise is biased towards an attractor state. For the binary encoding we assume the global attractor to be $|00\dots 0\rangle_{\ell n}$.

In this encoding, permutation of the integer label of a given variable corresponds to permutation of the computational basis vectors such that the set of gauge transformation is given by an n -fold tensor product of $2^\ell \times 2^\ell$ permutation matrices. Arbitrary basis permutations

can be compiled into reversible classical circuits, generally requiring multi-controlled gates or their decompositions. However, the subgroup of affine transformations ($x \mapsto Ax+b$) can always be decomposed into only X and CNOT gates (after noting the necessary SWAP operation decomposes into 3 CNOTs), which can help satisfy the requirement of circuit remappings remaining practical.

Indeed, arbitrary permutations as gauge transformations may change the form of the resulting cost Hamiltonian, and resulting circuit for the case of algorithms such as QAOA. For example, consider the gauge transformation $U = \text{SWAP}_{12}$ applied to a binary register. A term $Z_2 Z_3$ in the cost Hamiltonian will transform as $U^\dagger Z_2 Z_3 U = Z_1 Z_3$, which is more than just a coefficient sign change, and may for example introduce swaps or other changes to the hardware-level quantum circuit.

Fortunately, in binary encodings there always exists a set of gauge transformations of size k^n (i.e., one-to-one with integer strings) that only affects the signs of terms in the cost Hamiltonian - these are precisely those generated by products of ℓn bitflip Pauli X operators, that correspond to flipping the bits that differ between the physical attractor and encoded target string. Logically, this amounts to the affine transformation $x \mapsto x \oplus y$ bitwise, represented by the qubit gauge transformation

$$V(y) = \bigotimes_{v=1}^n \bigotimes_{j=0}^{\ell-1} X_{v_j}^{y_{v_j}}, \quad (18)$$

where the variable y_{v_j} is the difference between the j th color bit for vertex v in y and that of the attractor. This shows that we can always pick a compatible gauge transformation that decomposes into purely bit flips. The same logic as for bitflip transforms in the binary case then implies that this choice of $V(y)$ leaves the cost Hamiltonian the same up to signs of terms as desired.

Outlook: Integer problems encoded in binary appear compatible and attractive for NDAR as our preliminary analysis demonstrates, at least for the case where k is a power of 2. Binary encoding allows space efficient representation of the problem domain. The primary tradeoff is the requirement of $2\lceil \log k \rceil$ -local terms in the cost Hamiltonian and phase operator; fortunately, compilations to 2-local gates exist [44], and indeed this requirement has not been a major limitation in other results for quantum gate-model approaches [3], [45]. When $k \neq 2^\ell$ the assessment ultimately depends on details of the particular encoding or repair conventions employed.

Remark 2. Equation (15) considers a standard binary encoding; the insights of this section similarly apply to other related variants such as Gray codes [21].

B. Unary qubit encodings

Here we contrast three variants of unary encodings, which require $\sim k$ qubits per integer variable. These

encodings treat different k values uniformly, but come with additional (exponentially larger) qubit overhead.

1) *One-hot encoding:* In standard one-hot encoding we use k qubits per vertex to encode each color. We identify the k logical basis states of Eq. 11 with the k basis states of Hamming weight one

$$|10 \dots 00\rangle, |01 \dots 00\rangle, \dots |00 \dots 01\rangle. \quad (19)$$

Restricted to this valid subspace the cost Hamiltonian is 2-local and can be expressed [46, Eqn. 6.22] as

$$C = \frac{k|E|}{4} - \frac{1}{4} \sum_{(uv) \in E} \sum_{j=0}^{k-1} Z_{u,j} Z_{v,j}. \quad (20)$$

QAOA for this problem and encoding is detailed in [3]. The phase operator decomposes into at most $2k|E|$ CNOT gates. For this encoding, qubit XY mixers of the form $U_M(\beta) = \prod_{j=a}^k U_{M,a}(\beta)$ with

$$U_{M,j}(\beta) = \prod_{ij \in S(a)} \exp(-i\beta X_i X_j) \exp(-i\beta Y_i Y_j)$$

are proposed, which preserve qubit Hamming weight for each of the encoded qudits and hence never map valid to invalid states. Here the possible index set $S(a)$ for the qubits of each encoded variable includes both ring and fully-connected topologies, among others [3], [47].

NDAR: A practical difficulty with this scheme is that noise in general will cause leakage of probability amplitude out of the feasible subspace, and hence some fraction of measurement outcomes will yield invalid strings. For each logical qudit, the valid states are an exponentially small fraction of the encoded Hilbert space with respect to increasing k . Hence an attractor state is unlikely to correspond to a valid solution. (If the attractor was known to be a basis state of Eq. 19, then this case is logically equivalent to the qudit encoding of Sec. III, and our criteria would be satisfied such that we could proceed with NDAR as usual.) Indeed, our motivating attractor $|000 \dots 000\rangle$ is invalid for standard one-hot encodings. The next encoding we consider augments the logical one-hot subspace to include the $|00 \dots 0\rangle$ state.

2) *Augmented “01-hot” encoding:* Consider a variant of one-hot encoding where we use $k-1$ qubits per vertex instead of k to encode each color by also including the $|00 \dots 0\rangle$ state to encode the first color. Such an encoding was considered in [3]. Here we identify the logical basis states of Eq. 11 with the $1 + (k-1)$ qubit basis states

$$|00 \dots 00\rangle, |10 \dots 00\rangle, |01 \dots 00\rangle, \dots, |00 \dots 01\rangle$$

NDAR: The color corresponding to $|00 \dots 0\rangle$ is indicated by the projector $2^{-(k-1)} \prod_{i=0}^{k-2} (I + Z_{v_i})$, which contains a number of terms that grows exponentially with k and having locality up to $k-1$. Hence detecting (in)equality of two zero-color states introduces the product of indicators over both registers, yielding

up to $2(k-1)$ -local terms for the cost operators in general. On the other hand, one can always compile phase operators by again computing string inequality in an ancilla scratchpad register, performing phase kickback, and then uncomputing the ancilla qubits [19], [44].

Hence, in this encoding, the infeasible attractor issue goes away, and one can proceed with NDAR at the meta algorithm level. The catch is that the cost Hamiltonian and corresponding phase operator transform in a nontrivial way and are no longer 2-local. Hence this encoding may be suitable for, e.g., hardware-efficient ansätze (that don't depend on H), but less so for QAOA.

3) *Domain-wall encoding*: Consider instead the *domain-wall* encoding of [17] where we also use $k-1$ qubits per vertex to encode each color. Here we identify the logical basis states of Eq. (11) with the k basis states

$$|000\dots 00\rangle, |100\dots 00\rangle, |110\dots 00\rangle, \dots, |111\dots 11\rangle,$$

i.e. k colors are encoded in $k-1$ qubits as $r \rightarrow \mathcal{E}(r) := |1^r 0^{k-1-r}\rangle$, $r = 0, 1, \dots, k-1$. Here, again assuming we are restricted to the subspace of valid states, value indicator operators correspond to terms of the form $Z_i - Z_j$ or $I - Z_i$, such that 2-local qudit cost Hamiltonians are mapped to 2-local (QUBO) Hamiltonians and phase operators on qubits. Explicit derivations are shown in [17] by considering the action on the logical subspace. For QAOA mixers, Hamiltonian terms of the form $Z_i X_j - X_i Z_j$ and $\pm X_j$ are shown to be sufficient (in the sense of the QAOA mixer design criteria of [3]).

Gauge transforms: Here we propose the prefix-flip gauge as a natural choice: for target $\mathbf{y} \in \mathbb{Z}_k^n$ let

$$P_{\mathbf{y}} := \bigotimes_{i=1}^n \bigotimes_{j=1}^{y_i} X_{i,j}. \quad (21)$$

It is easy to verify this satisfies $P_{\mathbf{y}}|00\dots 0\rangle = |\mathcal{E}(\mathbf{y})\rangle$ as desired. On Pauli strings, prefix-flip gauges again act only by sign changes. Hence a domain-wall cost Hamiltonian retains the same Pauli support and locality after remapping. However, individual domain-wall value indicators, being linear combinations of I and Z_i , are not generally multiplied by an overall sign nor mapped to identical qubit operators but may transform to other diagonal operators of the same locality.

NDAR: In this encoding the presumed physical qubit attractor state $|00\dots 0\rangle$ is always valid, and one can proceed with NDAR at the meta algorithm level.

Outlook: Of the unary encodings considered, domain-wall presents the best suitability for NDAR with advantages over both one-hot encoding and the 01-hot variant. Nevertheless for all unary encoding noise is likely to lead to invalid strings, and hence they remain less attractive than qudit-native, or binary encodings when applicable.

C. Tradeoffs between quantum encodings

We summarize the tradeoffs between the different encodings considered for Max- k -colorable subgraph in

Table I above. The top of the table contrasts qudit with binary and unary qubit encodings in terms of resources and general suitability for NDAR. While both one-hot and domain-wall encodings always produce feasible solutions in the ideal limit (assuming a feasibility-preserving quantum circuit [3]), in practice noise and other types of errors will reduce this probability to be less than one. Binary encodings on the other hand have the desirable property that all strings are feasible, natively when k is a power of 2. For incorporating NDAR, four out of the five encodings considered have the desirable property that the $|00\dots 0\rangle$ state corresponds to a valid assignment.

The bottom two rows of the table show tradeoffs for applying an algorithm like QAOA using these encodings. While a binary encoding uses less space, it requires higher locality operators for the cost Hamiltonian and phase operator than the unary encodings. Additional complications arise when k is not a power of 2. For arbitrary k the locality becomes $2\lceil \log_2 k \rceil$, whereas the unary encoding cost operators remain 2-local. Note that on gate-model devices arbitrary ℓ -local interactions can be compiled to two-qubit gates, sometimes by incorporating additional ancilla qubits, but with circuit depth proportional to ℓ [44]. Still, the case is not so clear cut as all encodings have a number of terms that scale linearly with k .

The observations here illustrate that tradeoffs between different encodings are not always so clear cut, in particular for problems with modest k or problem size, and especially when one seeks to incorporate NDAR. This is reflected in the literature where different encodings are employed in different use cases. Hence, our results above may prove useful for incorporating NDAR across a wider variety of experiments in the near term.

V. DISCUSSION

In this work we extended the NDAR meta-algorithm beyond unconstrained binary optimization to integer-domain problems on both qudit-native and qubit-encoded hardware, including classes of problems with hard constraints. Treating both axes within a single framework opens NDAR to substantially broader applicability — and, critically, to a substantial fraction of emerging quantum hardware beyond the qubit paradigm. Our prototypical example, graph k -coloring, already illustrates the central tension between encodings: qudit-native ($d = k$) and qubit-encoded realizations are theoretically close cousins but differ qualitatively in feasibility, gauge structure, and circuit cost when integrated with NDAR. As summarized in Table I, we find qudit-native encodings to be the best fit when available. For qubits, while binary encodings appear favorable in particular cases, domain-wall encodings are applicable for all d and present relative advantages over the other qubit encodings considered in terms of NDAR.

Three findings drive most of our conclusions. First, NDAR's four ingredients (Sec. II-B) are aligned natively, not incidentally, with 3D superconducting cavity-based

qudit processors: cavity photon loss is well-modeled by the generalized amplitude damping channel, so the noise picture underlying NDAR appears to be well-matched to actual device noise [15], not purely an idealization. Second, the d -level qudit gauge multiplicity $((d-1)!)^n$ is a design lever rather than a defect: among compatible gauge transformations, one can *select* the cheapest to implement on the available hardware [38], a freedom absent in the qubit case. Third, among the encodings we considered, only the qudit-native encoding gives an *always-feasible* attractor with no encoding-induced invalid subspace, placing it on a different footing from binary, one-hot, and domain-wall qubit encodings even when their bare circuit costs may otherwise look comparable.

This paper is the algorithmic follow-up to a roadmap recently put forward in [16], where NDAR-QAOA on graph coloring was identified as the near-term optimization workload best matched to emerging superconducting cavity qudit processors [7]–[13], [48]. Two open theoretical questions were flagged there: how NDAR generalizes when the bitflip group is replaced by a richer gauge structure, and how qudit-native encodings compare to qubit encodings of the same integer problem. The framework of Sec. III–IV answers both. The hardware side has moved in parallel. The SQMS Center’s recently reported two-mode TESLA-geometry processor [49] demonstrates the NDAR-relevant regime concretely, with single-photon lifetimes $T_1 \simeq 20$ ms, Ramsey $T_2 > 20$ ms, and Fock-state preparation up to $|20\rangle$ at fidelity above 95% [15] via sideband feedforward and parity-filter post-selection. Algorithm-agnostic benchmarks [14] corroborate that contemporary transmons can drive a few tens of Fock levels at these coherence parameters, placing a useful working bound $d \lesssim 20$ on the per-mode dimension addressable today. A hardware demonstration of NDAR-QAOA nevertheless requires two R&D pushes:

(i) *High-fidelity two-qudit entangling gates* in the cavity-transmon architecture [22], [50]. The controlled-SUM (CSUM) gate is the natural phase-separator primitive but remains the central synthesis-and-calibration challenge on multimode cavities. Several primitive families are converging on this target. On the Gaussian side, parametric beamsplitter gates between cavity modes have reached 99.92% raw (99.98% leakage-detected) fidelity using parity-protected couplers [51], and ancilla-mediated extensions promote them to entangling gates with simulated error rates below 10^{-4} [52]. Sideband-based control of multimode memories has been pushed $30\times$ beyond the dispersive limit, enabling fast cavity–cavity SWAPs in 10-mode devices with millisecond-scale photon lifetimes [53]. Most directly relevant to NDAR-QAOA, the same SQMS platform of [15] provides an explicit qutrit CSUM blueprint synthesized from five virtual-Raman beamsplitter operations together with single-qutrit rotations, with simulated process fidelity $\sim 99\%$. A

complementary universal primitive in the weak-dispersive regime is Echoed Conditional Displacement (ECD) [40], whose multimode generalization, the Conditional-NOT-Displacement (CNOD) gate, entangles modes of a single multimode cavity through one weakly coupled transmon roughly two orders of magnitude faster than the dispersive limit [41], with optimal-control pulse shaping further reducing residual coherent errors [42]. ECD-based variational ansätze have already been demonstrated experimentally on cavity-transmon hardware [54], providing a concrete template for how NDAR-QAOA could be compiled in practice. Crucially, the qudit mixer of Eq. 13 often maps onto *unconditional* cavity displacements that bypass the transmon ancilla altogether, while the diagonal phase separator is generated by the natural cross-Kerr evolution at (in principle) no gate cost [22]. Combined with CSUM-style entanglers for non-quadratic (clock-shift) cost terms, ECD/CNOD and beamsplitter primitives thus form a near-complete native gate set for QAOA on Fock-encoded cavity qudits.

(ii) *Error suppression and gauge-aware compilation.* NDAR is beneficial when the dominant noise has a stable, characterizable bias. Dephasing-dominated or higher-temperature regimes weaken the attractor picture, and on encoded variables noise can cause leakage from the feasible subspace. Suppressing non-damping components of device noise via dynamical-decoupling sequences, randomized compiling, or partial error-correction on either the transmon or cavity modes [55]–[57] is therefore complementary to NDAR, particularly given recent evidence that NDAR can be negatively impacted by residual dephasing [58], [59]. Quantum error correction and fault-tolerant resource assessments for qudits remain active adjacent areas offering further sophistications [31], [60]–[64].

Beyond these two priorities the framework opens broader directions. While here we focused on integer domains and constraints induced by encoding, NDAR appears amenable to extending to other discrete domains (e.g. permutations, for problems such as the Traveling Salesperson) and further tailoring to specific classes of hard constraint. In ongoing related work [59] we are developing a new meta-algorithm that combines NDAR with iterative warm-starts [65]–[68]; the results of this paper port directly to that setting. Recent follow-on work has shown further improvements to NDAR are possible via additional classical processing [58], [69], and these insights should similarly carry over. More speculatively, better leveraging open-system and thermodynamic considerations, whether algorithmic [70], [71] or physical (Sec. III-A), is an attractive direction for principled algorithm modifications.

ACKNOWLEDGMENTS

We are grateful for helpful discussion with Tanay Roy, Silvia Zorzetti, Doga Kürkçüoğlu, and Daniel

Koch. We acknowledge support from NASA (ISRDS contract 80ARC020D0010) and Department of Energy, Office of Science, National Quantum Information Science Research Centers, Superconducting Quantum Materials and Systems Center (SQMS), under Contract No. 89243024CSC000002, and grant No. DE-SC0026126; and from AFRL Contract No. FA8750-25-C-B0040.

REFERENCES

- [1] F. B. Maciejewski, J. Biamonte, S. Hadfield, and D. Venturelli, “Improving quantum approximate optimization by noise-directed adaptive remapping,” *Quantum*, vol. 9, p. 1906, 2025.
- [2] E. Farhi, J. Goldstone, and S. Gutmann, “A quantum approximate optimization algorithm,” *arXiv preprint arXiv:1411.4028*, 2014.
- [3] S. Hadfield, Z. Wang, B. O’gorman, E. G. Rieffel, D. Venturelli, and R. Biswas, “From the quantum approximate optimization algorithm to a quantum alternating operator ansatz,” *Algorithms*, vol. 12, no. 2, p. 34, 2019.
- [4] D. D. Awschalom, H. Bernien, R. Hanson, W. D. Oliver, and J. Vučković, “Challenges and opportunities for quantum information hardware,” *Science*, vol. 390, no. 6777, pp. 1004–1010, 2025.
- [5] A. Abbas, A. Ambainis, B. Augustino, A. Bärttschi, H. Buhрман, C. Coffrin, G. Cortiana, V. Dunjko, D. J. Egger, B. G. Elmegreen, *et al.*, “Challenges and opportunities in quantum optimization,” *Nature Reviews Physics*, pp. 1–18, 2024.
- [6] Y. Wang, Z. Hu, B. C. Sanders, and S. Kais, “Qudits and high-dimensional quantum computing,” *Frontiers in Physics*, vol. 8, p. 589504, 2020.
- [7] Q.-P. Su, T. Liu, Y. Zhang, and C.-P. Yang, “Construction of a qudit using schrödinger cat states and generation of hybrid entanglement between a discrete-variable qudit and a continuous-variable qudit,” *Physical Review A*, vol. 104, no. 3, p. 032412, 2021.
- [8] M. S. Blok, V. V. Ramasesh, D. I. Schuster, and I. Siddiqi, “Quantum information scrambling on a superconducting qutrit processor,” *Physical Review X*, vol. 11, p. 021010, 2021.
- [9] Y. Chi, J. Huang, Z. Zhang, J. Mao, Z. Zhou, X. Chen, C. Zhai, J. Bao, T. Dai, H. Yuan, *et al.*, “A programmable qudit-based quantum processor,” *Nature communications*, vol. 13, no. 1, p. 1166, 2022.
- [10] M. Ringbauer, M. Meth, L. Postler, R. Stricker, I. Pogorelov, B. P. Lanyon, R. Blatt, and T. Monz, “Universal qudit quantum computation with trapped ions,” *Nature Physics*, vol. 18, pp. 1053–1057, 2022.
- [11] T. Roy, Z. Li, E. Kapit, and D. Schuster, “Two-qutrit quantum algorithms on a programmable superconducting processor,” *Physical Review Applied*, vol. 19, no. 6, p. 064024, 2023.
- [12] A. Denys and A. Leverrier, “The $2t$ -qutrit, a two-mode bosonic qutrit,” *Quantum*, vol. 7, p. 1032, 2023.
- [13] L. B. Nguyen, N. Goss, K. Siva, Y. Kim, E. Younis, B. Qing, A. Hashim, D. I. Santiago, and I. Siddiqi, “Empowering a qudit-based quantum processor by traversing the dual bosonic ladder,” *Nature Communications*, vol. 15, no. 1, p. 7117, 2024.
- [14] N. Bornman, T. Roy, J. A. Job, N. Anand, G. N. Perdue, S. Zorzetti, and M. S. Alam, “Benchmarking the performance of a high-q cavity qudit using random unitaries,” *Quantum Science and Technology*, vol. 10, no. 2, p. 025062, 2025.
- [15] T. Kim, T. Roy, X. You, A. C. Li, H. Lamm, O. Pronitchev, M. Bal, S. Garattoni, F. Crisa, D. Bafia, *et al.*, “Ultracoherent superconducting cavity-based multiqudit platform with error-resilient control,” *arXiv preprint arXiv:2506.03286*, 2025.
- [16] D. Venturelli, E. Gustafson, D. Kurkcuoglu, and S. Zorzetti, “Near-term application engineering challenges in emerging superconducting qudit processors,” *arXiv preprint arXiv:2506.05608*, 2025.
- [17] N. Chancellor, “Domain wall encoding of discrete variables for quantum annealing and qaoa,” *Quantum Science and Technology*, vol. 4, no. 4, p. 045004, 2019.
- [18] A. Lucas, “Ising formulations of many NP problems,” *Frontiers in physics*, vol. 2, p. 5, 2014.
- [19] S. Hadfield, “On the representation of Boolean and real functions as hamiltonians for quantum computing,” *ACM Transactions on Quantum Computing*, vol. 2, p. 1–21, Dec. 2021.
- [20] S. Bravyi, A. Kliesch, R. Koenig, and E. Tang, “Hybrid quantum-classical algorithms for approximate graph coloring,” *Quantum*, vol. 6, p. 678, 2022.
- [21] N. P. Sawaya, A. T. Schmitz, and S. Hadfield, “Encoding trade-offs and design toolkits in quantum algorithms for discrete optimization: coloring, routing, scheduling, and other problems,” *Quantum*, vol. 7, p. 1111, Sept. 2023.
- [22] A. B. Özgüler and D. Venturelli, “Numerical gate synthesis for quantum heuristics on bosonic quantum processors,” *Frontiers in Physics*, vol. 10, p. 900612, 2022.
- [23] Y. Deller, S. Schmitt, M. Lewenstein, S. Lenk, M. Federer, F. Jendrzejewski, P. Hauke, and V. Kasper, “Quantum approximate optimization algorithm for qudit systems,” *Physical Review A*, vol. 107, no. 6, p. 062410, 2023.
- [24] A. Apte, S. Boulebnane, Y. Jin, S. Omanakuttan, M. A. Perlin, and R. Shaydulin, “Quantum approximate optimization of integer graph problems and surpassing semidefinite programming for max-k-cut,” *arXiv preprint arXiv:2602.05956*, 2026.
- [25] I. L. Chuang, D. W. Leung, and Y. Yamamoto, “Bosonic quantum codes for amplitude damping,” *Physical Review A*, vol. 56, no. 2, p. 1114, 1997.
- [26] M. Grassl, L. Kong, Z. Wei, Z.-Q. Yin, and B. Zeng, “Quantum error-correcting codes for qudit amplitude damping,” *IEEE Transactions on Information Theory*, vol. 64, no. 6, pp. 4674–4685, 2018.
- [27] S. Dutta, D. Biswas, and P. Mandayam, “Noise-adapted qudit codes for amplitude-damping noise,” *Physical Review A*, vol. 111, no. 3, p. 032438, 2025.
- [28] C. J. Wood and J. M. Gambetta, “Quantification and characterization of leakage errors,” *Physical Review A*, vol. 97, no. 3, p. 032306, 2018.
- [29] B. Li, F. Cárdenas-López, A. Lupascu, and F. Motzoi, “Universal pulses for superconducting qudit ladder gates,” *PRX Quantum*, vol. 6, no. 3, p. 030357, 2025.
- [30] G. Ausiello, P. Crescenzi, G. Gambosi, V. Kann, A. Marchetti-Spaccamela, and M. Protasi, *Complexity and approximation: Combinatorial optimization problems and their approximability properties*. Springer Science & Business Media, 2012.
- [31] E. Hostens, J. Dehaene, and B. De Moor, “Stabilizer states and clifford operations for systems of arbitrary dimensions and modular arithmetic,” *Physical Review A*, vol. 71, no. 4, p. 042315, 2005.
- [32] T. Proctor, M. Giulian, N. Korolkova, E. Andersson, and V. Kendon, “Ancilla-driven quantum computation for qudits and continuous variables,” *Physical Review A*, vol. 95, no. 5, p. 052317, 2017.
- [33] E. M. Murairi, M. S. Alam, H. Lamm, S. Hadfield, and E. Gustafson, “Highly-efficient quantum fourier transformations for certain non-abelian groups,” *Physical Review D*, vol. 110, no. 7, p. 074501, 2024.
- [34] S. Yang, L. Xu, G. Tian, and X. Sun, “Quantum circuit synthesis with qudit phase gadget method,” *arXiv preprint arXiv:2504.12710*, 2025.
- [35] S. Krastanov, V. V. Albert, C. Shen, C.-L. Zou, R. W. Heeres, B. Vlastakis, R. J. Schoelkopf, and L. Jiang, “Universal control of an oscillator with dispersive coupling to a qubit,” *Physical Review A*, vol. 92, no. 4, p. 040303, 2015.
- [36] R. W. Heeres, B. Vlastakis, E. Holland, S. Krastanov, V. V. Albert, L. Frunzio, L. Jiang, and R. J. Schoelkopf, “Cavity state manipulation using photon-number selective phase gates,” *Physical review letters*, vol. 115, no. 13, p. 137002, 2015.
- [37] J. Job, “Efficient, direct compilation of su(n) operations into snap & displacement gates,” *arXiv preprint arXiv:2307.11900*, 2023.
- [38] D. M. Kürkçüoğlu, H. Lamm, and A. Maestri, “Qudit gate decomposition dependence for lattice gauge theories,” *arXiv preprint arXiv:2410.16414*, 2024.
- [39] O. Ogunkoya, K. Morris, and D. M. Kürkçüoğlu, “Investigating parameter trainability in the snap-displacement protocol of a qudit system,” *Physica Scripta*, vol. 100, no. 7, p. 075109, 2025.
- [40] A. Eickbusch, V. Sivak, A. Z. Ding, S. S. Elder, S. R. Jha, J. Venkatraman, B. Royer, S. M. Girvin, R. J. Schoelkopf, and

- M. H. Devoret, "Fast universal control of an oscillator with weak dispersive coupling to a qubit," *Nature Physics*, vol. 18, no. 12, pp. 1464–1469, 2022.
- [41] A. A. Diringer, E. Blumenthal, A. Grinberg, L. Jiang, and S. Hacoheh-Gourgy, "Conditional-not displacement: Fast multioscillator control with a single qubit," *Physical Review X*, vol. 14, no. 1, p. 011055, 2024.
- [42] M. Lapointe-Major *et al.*, "Optimizing pulse shapes of an echoed conditional displacement gate in a superconducting bosonic system," *arXiv preprint arXiv:2408.05299*, 2024.
- [43] A. B. Özgüler and J. A. Job, "Dynamics of qudit gates and effects of spectator modes on optimal control pulses," *Physical Review A*, vol. 109, no. 5, p. 052404, 2024.
- [44] A. Barenco, C. H. Bennett, R. Cleve, D. P. DiVincenzo, N. Margolus, P. Shor, T. Sleator, J. A. Smolin, and H. Weinfurter, "Elementary gates for quantum computation," *Physical review A*, vol. 52, no. 5, p. 3457, 1995.
- [45] R. Shaydulin, C. Li, S. Chakrabarti, M. DeCross, D. Herman, N. Kumar, J. Larson, D. Lykov, P. Minssen, Y. Sun, *et al.*, "Evidence of scaling advantage for the quantum approximate optimization algorithm on a classically intractable problem," *Science Advances*, vol. 10, no. 22, p. eadm6761, 2024.
- [46] S. A. Hadfield, *Quantum algorithms for scientific computing and approximate optimization*. Columbia University, 2018.
- [47] Z. Wang, N. C. Rubin, J. M. Dominy, and E. G. Rieffel, "Xy mixers: Analytical and numerical results for the quantum alternating operator ansatz," *Physical Review A*, vol. 101, no. 1, p. 012320, 2020.
- [48] P. Gokhale, J. M. Baker, C. Duckering, N. Brown, K. R. Brown, and F. T. Chong, "Asymptotic improvements to quantum circuits via qutrits," in *Proceedings of the 46th International Symposium on Computer Architecture (ISCA)*, pp. 554–566, ACM, 2019.
- [49] A. Reineri, S. Zorzetti, T. Roy, and X. You, "Exploration of superconducting multi-mode cavity architectures for quantum computing," in *2023 IEEE International Conference on Quantum Computing and Engineering (QCE)*, vol. 1, pp. 1342–1348, IEEE, 2023.
- [50] Y. Liu, S. Singh, K. C. Smith, E. Crane, J. M. Martyn, A. Eickbusch, A. Schuckert, R. D. Li, J. Sinanan-Singh, M. B. Soley, *et al.*, "Hybrid oscillator-qubit quantum processors: Instruction set architectures, abstract machine models, and applications," *arXiv preprint arXiv:2407.10381*, 2024.
- [51] Y. Lu, A. Maiti, J. W. O. Garmon, S. Ganjam, Y. Liu, J. Cao, B. J. Chapman, T. Tsunoda, A. Eickbusch, R. J. Schoelkopf, and M. H. Devoret, "High-fidelity parametric beamsplitting with a parity-protected converter," *Nature Communications*, vol. 14, p. 5767, 2023.
- [52] T. Tsunoda, J. D. Teoh, W. D. Kalfus, S. Rosenblum, A. Eickbusch, N. E. Frattini, P. Reinhold, R. J. Schoelkopf, M. H. Devoret, L. Jiang, and S. M. Girvin, "Error-detectable bosonic entangling gates with a noisy ancilla," *PRX Quantum*, vol. 4, no. 2, p. 020354, 2023.
- [53] Y. Huang, S. DiNapoli, G. Rockwood, A. Vrajitoarea, S. Boutin, W.-L. Ma, T. Roy, and S. Chakram, "Fast sideband control of a weakly coupled multimode bosonic memory," *arXiv preprint arXiv:2503.10623*, 2025.
- [54] R. Dutta, N. Cao, A. Bhattacharyya, J. Mead, A. Pal, *et al.*, "Simulating electronic structure on bosonic quantum computers," *Journal of Chemical Theory and Computation*, vol. 21, p. 2281, 2025.
- [55] V. Tripathi, N. Goss, A. Vezvaea, L. B. Nguyen, I. Siddiqi, and D. A. Lidar, "Qudit dynamical decoupling on a superconducting quantum processor," *Physical Review Letters*, vol. 134, no. 5, p. 050601, 2025.
- [56] N. Suri, J. Saied, and D. Venturelli, "Uniformly decaying subspaces for error-mitigated quantum computation," *Physical Review A*, vol. 110, no. 4, p. 042621, 2024.
- [57] S. Dambal, A. Sone, and Y. Zhang, "Harnessing intrinsic noise for quantum simulation of open quantum systems," *arXiv preprint arXiv:2510.21075*, 2025.
- [58] W.-H. Tam, H. Matsuyama, R. Sakai, and Y. Yamashiro, "Enhancing ndar with delay-gate-induced amplitude damping," *arXiv preprint arXiv:2504.12628*, 2025.
- [59] F. Maciejewski, S. Hadfield, O. Wallis, G. Pennington, S. Brandhofer, S. Woerner, D. J. Egger, and D. Venturelli, "Quantum approximate optimization via noise-directed adaptive warm-starting," *arXiv (to appear)*, 2026.
- [60] E. Knill, "Non-binary unitary error bases and quantum codes," *arXiv preprint quant-ph/9608048*, 1996.
- [61] D. Gottesman, "Fault-tolerant quantum computation with higher-dimensional systems," *Chaos, Solitons & Fractals*, vol. 10, no. 10, pp. 1749–1758, 1999.
- [62] A. Ashikhmin and E. Knill, "Nonbinary quantum stabilizer codes," *IEEE Transactions on Information Theory*, vol. 47, no. 7, pp. 3065–3072, 2001.
- [63] S. S. Bullock and G. K. Brennen, "Qudit surface codes and gauge theory with finite cyclic groups," *Journal of Physics A: Mathematical and Theoretical*, vol. 40, no. 13, p. 3481, 2007.
- [64] S. Godwood, D. M. Kürkçüoğlu, G. N. Perdue, M. Maneyro, and A. Roggero, "Fault-tolerant resource comparison of qudit and qubit encodings for diagonal quadratic operators," *arXiv preprint arXiv:2604.26792*, 2026.
- [65] D. J. Egger, J. Mareček, and S. Woerner, "Warm-starting quantum optimization," *Quantum*, vol. 5, p. 479, 2021.
- [66] M. A. Lopez-Ruiz, E. L. Tucker, E. M. Arnold, E. Epifanovsky, A. Kaushik, and M. Roetteler, "A non-variational quantum approach to the job shop scheduling problem," *arXiv preprint arXiv:2510.26859*, 2025.
- [67] K. V. Marshall, D. J. Egger, M. Garn, F. Schiavello, S. Brandhofer, C. Zoufal, and S. Woerner, "Quantum-enhanced markov chain monte carlo for combinatorial optimization," *arXiv preprint arXiv:2602.06171*, 2026.
- [68] P. C. Lotshaw, T. Morris, S. Hadfield, and R. Bennink, "Iterative warm-start optimization with quantum imaginary time evolution," *arXiv preprint arXiv:2604.26047*, 2026.
- [69] F. B. Maciejewski, B. G. Bach, M. Dupont, P. A. Lott, B. Sundar, D. E. B. Neira, I. Safro, and D. Venturelli, "A multilevel approach for solving large-scale qubo problems with noisy hybrid quantum approximate optimization," in *2024 IEEE High Performance Extreme Computing Conference (HPEC)*, pp. 1–10, IEEE, 2024.
- [70] P. Díez-Valle, D. Porras, and J. J. García-Ripoll, "Quantum approximate optimization algorithm pseudo-boltzmann states," *Physical review letters*, vol. 130, no. 5, p. 050601, 2023.
- [71] P. C. Lotshaw, G. Siopsis, J. Ostrowski, R. Herrman, R. Alam, S. Powers, and T. S. Humble, "Approximate boltzmann distributions in quantum approximate optimization," *Physical Review A*, vol. 108, no. 4, p. 042411, 2023.